The nonlinear optical properties of a magneto-exciton in a strained $Ga_{0.2}In_{0.8}As/GaAs$ quantum dot

N. R. Senthil Kumar[a], A. John Peter[b]†, and Chang Kyoo Yoo[c]

[a] *Department of Physics, SBM College of Engineering and Technology, Dindigul-624 005, India*
[b] *Department of Physics, Govt. Arts College, Melur-625 106, Madurai, India*
[c] *Center for Environmental Studies/Green Energy Center, Deptartment of Environmental Science and Engineering, College of Engineering, Kyung Hee University, Seocheon-dong 1, Giheung-gu, Yongin-Si, Gyeonggi-Do, 446-701, South Korea*

(Received 3 March 2013; revised manuscript received 3 April 2013)

The magnetic field-dependent heavy hole excitonic states in a strained $Ga_{0.2}In_{0.8}As/GaAs$ quantum dot are investigated by taking into account the anisotropy, non-parabolicity of the conduction band, and the geometrical confinement. The strained quantum dot is considered as a parabolic dot of InAs embedded in a GaAs barrier material. The dependence of the effective excitonic *g*-factor as a function of dot radius and the magnetic field strength is numerically measured. The interband optical transition energy as a function of geometrical confinement is computed in the presence of a magnetic field. The magnetic field-dependent oscillator strength of interband transition under the geometrical confinement is studied. The exchange enhancements as a function of dot radius are observed for various magnetic field strengths in a strained $Ga_{0.2}In_{0.8}As/GaAs$ quantum dot. Heavy hole excitonic absorption spectra, the changes in refractive index, and the third-order susceptibility of third-order harmonic generation are investigated in the $Ga_{0.2}In_{0.8}As/GaAs$ quantum dot. The result shows that the effect of magnetic field strength is more strongly dependent on the nonlinear optical property in a low-dimensional semiconductor system.

Keywords: oscillator strength, exciton, quantum dot

PACS: 71.70.Di, 72.20.Ht, 73.20.Hb, 73.21.La **DOI:** 10.1088/1674-1056/22/10/107106

1. Introduction

The quantum size effects are quite interesting in low-dimensional semiconductor systems and especially in quantum dots due to their discrete nature of density of states. Studies on quantum dots have received due attention because of their potential applications in device fabrication such as in opto-electronic devices and their properties that are found to have better optical and electrical characteristics.[1] As the size of a dot approaches its effective Bohr radius, the excitonic properties change and eventually a blue shift occurs in the interband optical transition energy.[2] Semiconducting quantum dots from group III–V have attracted attention because they have larger effective Bohr radii which are comparable to the dot sizes. This property can be used for fabricating laser diodes and infrared detectors.[3] Moreover, the electron and the hole are confined in all the three directions in a quantum dot and as a result of this geometrical confinement, an enhanced exciton binding energy and oscillator strength are observed. Further, the quantum dots show an atom-like spectrum of energy of a delta function[4] and the spectral lines will be split under an external magnetic field.[5]

The optical properties, especially the optical gain of an Er-doped Al_2O_3 waveguide amplifier in which the optical loss varies with annealing temperature, were studied by Tan and Zhang,[6] and it was found that the optical loss is a main parameter for determining the optical gain. Electronic and optical properties of III–V semiconductors especially InAs/GaAs quantum dots and coupled quantum dots[7–9] have been investigated. Preisler *et al.*[10] have investigated the interband transitions in several ensembles of self-assembled InAs/GaAs quantum dots by using photoluminescence excitation spectroscopy under a strong magnetic field. The geometrical sizes, shapes, and compositions of InAs/GaAs quantum dots have been investigated by Offermans *et al.*[11] using cross-sectional scanning tunneling microscopy. They used a single band effective mass approximation to compute the electron and hole states in order to find the ground state photoluminescence energy. The variation of strain has been investigated using elastic continuum theory in InAs/GaAs pyramidal dots in which a single band effective mass approach has been followed.[12] Theoretical approaches with the combined effects of electric field and hydrostatic pressure on the binding energy in a coupled InAs/GaAs quantum-well wire have been investigated.[13] Electron and hole levels, oscillator strengths, and the exciton ground-state binding energies in pyramid-shaped InAs quantum dots in GaAs were computed.[14] The exciton and the optical phonon in an InGaAs ternary alloy have been studied and compared with those in the II-VI semiconductors.[15–17] Some ternary quantum well structures including InGaAs semiconductors have been grown and the band-gap energy and higher state transition energy

†Corresponding author. E-mail: a.john.peter@gmail.com

© 2013 Chinese Physical Society and IOP Publishing Ltd

have been calculated by using a proper model.[18]

In the present work, we investigate the heavy hole excitonic states in a strained $Ga_xIn_{1-x}As/GaAs$ quantum dot in the presence of a magnetic field. The calculations include the anisotropy, non-parabolicity of the conduction band, and the geometrical confinement. The strained quantum dot is considered as a parabolic dot of InAs surrounded by a GaAs barrier material. The exciton effective Lande factor is measured as a function of dot radius and Ga alloy content in a $Ga_xIn_{1-x}As/GaAs$. The interband emission energy is computed with the spatial confinement and the external magnetic field strength. The exchange enhancements as a function of dot radius are studied in a strained $Ga_{0.2}In_{0.8}As/GaAs$ quantum dot for various magnetic field strengths. The oscillator strength of interband transitions under the spatial confinement in the InAs/GaAs quantum dot is investigated. Some nonlinear optical properties as a function of photon energy are dealt with. The rest of this paper is organized as follows. In Section 2, the theoretical model used in our calculations, and the obtained eigenfunctions and eigenenergies of exciton states, the interband emission energy and the nonlinear optical properties are discussed. The results and discussion are presented in Section 3. Finally, a brief summary and results are presented in the last section.

2. Model and calculations

2.1. Exciton binding energy

The Hamiltonian consists of an exciton in a $Ga_{0.2}In_{0.8}As$ quantum dot surrounded by a spherical potential barrier in GaAs material. The potential inside a dot is assumed to be zero and $V_0(B)$ outside. Based on the single band effective mass approximation, the Hamiltonian of a confined exciton in a $Ga_{0.2}In_{0.8}As/GaAs$ quantum dot is written as

$$\hat{H}_{\rm exc} = H_{\rm e} + H_{\rm h} - \frac{e^2}{\varepsilon|\bar{r}_{\rm e} - \bar{r}_{\rm h}|} + V_{\rm D}(r), \tag{1}$$

where e is the free electron charge, $|\bar{r}_{\rm e} - \bar{r}_{\rm h}|$ denotes the relative distance between the electron (e) and the hole (h), ε is the dielectric constant of the material inside the quantum dot, $V_{\rm D}(r)$ is the parabolic confinement potential given as $V_{\rm D}(r) = V_0(B)r^2/R^2$ for $|r| \le R$ while $V_{\rm D} = V_0(B)$ for $|r| > R$ with $V_0(B)$ being the barrier height of the parabolic dot and

$$V_0(B) = Q_{\rm c}\Delta E_{\rm g}^{\Gamma}(x) \tag{2}$$

being the barrier height ($V_{\rm c} = 288$ meV and $V_{\rm v} = 192$ meV, for $x = 0.2$). And in Eq. (2) $Q_{\rm c}$ is the conduction band offset parameter which is taken to be 60:40 between conduction band and valence band, and $\Delta E_{\rm g}^{\Gamma}(x)$ is the band gap difference between the quantum dot and the barrier at Γ-point, given by

$$\Delta E_{\rm g}^{\Gamma}(x) = 0.359 + 0.491x + 0.58x^2. \tag{3}$$

For any quantum semiconducting nanostructure, the effect of strain modifies the band structure which includes the conduction and the valence edge energies. Assuming homogenous strain in the epitaxial layer, we introduce the strain contribution into the Hamiltonian. Hydrostatic and uniaxial strains will be induced due to the lattice constant mismatch between different materials. The former will influence the lattice volume and result in a change in energy level of materials whereas the latter will remove the degeneracy. The strain-induced potential for the conduction band can be expressed as[19]

$$V_{\rm Cstrian} = a_{\rm c}(\varepsilon_{xx} + \varepsilon_{yy} + \varepsilon_{zz}), \tag{4}$$

where $a_{\rm c}$ is the deformation potential constant of conduction band, the strain tensor components defined as $\varepsilon_{xx} = \varepsilon_{yy} = (a_0 - a)/a$ where a_0 and a are the lattice parameters of bulk InAs and GaAs respectively and $\varepsilon_{zz} = -2(C_{12}/C_{11})\varepsilon_{xx}$ where C_{ij} are the elastic stiffness constants and their values are given in Table 1.

Table 1. Material parameters[a] used in the calculations (all the other parameters are linearly interpolated).

Parameter	InAs	GaAs	Unit
$E_{\rm g}$	0.418	1.517	eV
$m_{\rm e}$	0.023	0.067	m_0
ε	15.15	13.13	
γ_1	20	6.98	
γ_2	8.5	2.06	
C_{11}	83.29	11.88	GPa
C_{12}	45.26	5.38	GPa
C_{44}	23.0	5.94	GPa
$a_{\rm c}$	−5.08	−7.17	eV
$a_{\rm v}$	1	−1.16	eV
b	−1.8	2	eV
a	0.6058	0.565	nm
$E_{\rm p}$	22.2	25.7	eV
Δ_0	0.386	0.340	eV

[a]Cited from Refs. [35]–[39]

The strain-induced potential for the valence band can then be written as[25]

$$V_{\rm Vstrain} = a_{\rm v}(\varepsilon_{xx} + \varepsilon_{yy} + \varepsilon_{zz}) - \frac{b}{2}(\varepsilon_{xx} + \varepsilon_{yy} - 2\varepsilon_{zz}), \tag{5}$$

where $a_{\rm v}$ and b are the deformation potential constants of valence band for the hydrostatic components of the strain along $\langle 001 \rangle$ as given in Table 1.

The internal strain influences the electronic parameters, which are realized through an effective Lande factor (g-factor) here. The effective g-factor for electron (hole) having energy $E_{\rm c}\,(E_{\rm v})$ measured from the bottom (top) of the conduction (valence) band is given as

$$g(E,x) = 2 - \frac{2E_{\rm p}(x)\Delta(x)}{3(E_{\rm g}(x) + E)(E_{\rm g}(x) + E + \Delta(x))}. \tag{6}$$

Here, $E_{\rm g}(x)$ and $\Delta(x)$ are the Ga-dependent fundamental band gap energy and spin–orbit splitting energy respectively, $E_{\rm P}$ describes the coupling energy between the conduction band Γ_6

and valence bands Γ_7 and Γ_8 and the corresponding values are as shown in Table 1.

The heavy hole mass $m^*_{\rm hh}$ is given by

$$\frac{m_0}{m^*_{\rm hh}} = \gamma_1 - 2\gamma_2, \tag{7}$$

where m_0 is the free electron mass, γ_1 and γ_2 are the Luttinger parameters. The effect of band non-parabolicity is taken into consideration in our calculations through using the energy-dependent electron mass $m^*_{\rm NP}$ given as

$$m^*_{\rm NP} = m^*_{\rm e}(1+\alpha E), \tag{8}$$

where α is the material-dependent non-parabolicity parameter ($0.0025\ {\rm meV}^{-1}$ [26]). The lowest energy of the electron (hole), E, is obtained by solving the single particle Schrödinger equation using the electron (hole) bulk mass.

The electron (hole) effective mass, m^*_j, is given by

$$m^*_j = \begin{cases} m^*_{\rm I}, & r < R, \\ m^*_{\rm II}, & r \geq R, \end{cases} \tag{9}$$

where $m^*_{\rm I}$ and $m^*_{\rm II}$ denote the reduced effective mass of the inner dot and outer dot. The material parameters are given in Table 1.

The strain effect inducing an extra potential field is included in the present work. For the strained quantum dot nanostructure, the confinement potential is measured as the addition of energy offsets of the conduction band (or valence band) and the strain-induced potential in all the computations.

The Schrödinger wave equation for the exciton within the single band effective mass approximation is given by

$$H_{\rm exc}\Psi(r_{\rm e}, r_{\rm h}) = E_{\rm exc}\Psi(r_{\rm e}, r_{\rm h}), \tag{10}$$

where $E_{\rm exc}$ is the energy and ψ is the wave function for the eigen-energy of the system.

In the presence of a uniform magnetic field applied along the z direction, the single particle Hamiltonian is written as

$$H_{\rm e(h)} = -\sum_{i={\rm e,h}} \left(\frac{\hbar^2}{2m_i(E)} \left[\frac{\partial^2}{\partial r^2} + \frac{2}{r}\frac{\partial}{\partial r} \right] + V_{\rm D}(r_i) \right) - \frac{{\rm i}\hbar eB}{2m_i(E)c}\frac{\partial}{\partial \varphi} + \frac{e^2B^2r^2}{8m_i(E)c^2}. \tag{11}$$

The ground state energy of an electron (hole) in a parabolic quantum dot is estimated by variational method. We have assumed the trial functions to be[27]

$$\begin{aligned} \psi_{\rm in}(r) &= A_{\rm in}\,{\rm e}^{-\xi r2}, & r < R, \\ \psi_{\rm out}(r) &= -A_{\rm out}\frac{{\rm e}^{-\delta r}}{r}, & r \geq R. \end{aligned} \tag{12}$$

Here $A_{\rm in}$ and $A_{\rm out}$ are normalization constants. The wave functions and their derivatives at the boundaries of the quantum dot are matched in order to fix the values of normalization constants. The δ has been taken as the variational parameter in this problem. The ground state energy of the conduction electron (hole) in a parabolic quantum dot in the external magnetic field, $E_{\rm exc}$, is obtained by minimizing the expectation value of $H_{\rm exc}$ with respect to the variational parameter using Eq. (12). The exciton binding energy in the presence of magnetic field, $E_{\rm exc}(B) = E_{\rm e(h)}(B) + \gamma - \langle\psi|H_{\rm exc}|\rangle_{\rm min}$, is obtained by variational method using the following trial wave functions with β as the variational parameter

$$\begin{aligned} \psi_{\rm in(I)}(r) &= \psi_{\rm in}\,{\rm e}^{-\beta r}, & r < R, \\ \psi_{\rm out(I)}(r) &= \psi_{\rm out}\,{\rm e}^{-\beta r}, & r \geq R. \end{aligned} \tag{13}$$

The magnetic field-induced interband emission energy $E_{\rm ph}(B)$ associated with the exciton is calculated using the following equation:

$$E_{\rm ph}(B) = E_{\rm e} + E_{\rm h} + E_{\rm g} - E_{\rm exc}(B), \tag{14}$$

where $E_{\rm e}$ and $E_{\rm h}$ are the confinement energies of electron and hole respectively, and $E_{\rm g}$ is the band gap energy of $Ga_{0.2}In_{0.8}As$ material.

2.2. Nonlinear optical properties

The intensity of the exciton binding energy and the envelope wave function are characterized by the oscillator strength in any absorption spectrum.[28] The expression for the oscillator strength is given by

$$f = \frac{E_{\rm p}}{E_{\rm exc}} \left| \int_V \psi_{\rm exc}(r)\,{\rm d}r \right|^2, \tag{15}$$

where the $E_{\rm exc}$ is the exciton binding energy, $E_{\rm p}$ is the Kane energy of InAs, and $\psi_{\rm exc}$ is the exciton wave function. The oscillator strength increases with dot radius increasing. The radiative life time can be calculated as[29]

$$\tau = \frac{2\pi\varepsilon_0 m_0 c^3 h^2}{\sqrt{\varepsilon} e^2 E^2_{\rm exc} f}, \tag{16}$$

where f is the oscillator strength as given in Eq. (15) and all the other parameters are universal physical constants.

The results of oscillator strength and the radiative life time are important in calculating the various linear and nonlinear optical properties. On the other hand, the dipole transition occurring between two energy levels must obey the selection rules, i.e., $\Delta l = \pm 1$ where l is the angular momentum quantum number. Further, the oscillator strength associated with the dipole transition is given by

$$P_{fi} = \frac{2m*}{\hbar^2}\Delta E_{fi}\left|M_{fi}\right|^2, \tag{17}$$

where $\Delta E_{fi} = E_f - E_i$ denotes the difference in energy between the lower and upper states. The matrix element, $M_{fi} = 2\langle f|\boldsymbol{R}|i\rangle$ is defined as the electric dipole moment of the transition from i state to f state in the quantum dot. The matrix element is important for the calculation of different optical prop-

erties of the system related to the electronic transitions especially in low-dimensional semiconductor systems. The investigations of oscillator strength are important especially in the study of optical properties, which is related to the electronic dipole-allowed absorptions. In addition, the outcomes of the nonlinear optical properties will be viewed as being related to the fine structure of the optical absorption. Using the Fermi golden rule, from which the total absorption coefficient can be obtained, the expression for the optical absorption is given by[30]

$$\begin{aligned}\alpha(\omega,I) &= \alpha_1(\omega)+\alpha_3(\omega,I)\\ &= \omega\sqrt{\frac{\mu_0}{\varepsilon_r}}\mathrm{Im}[\varepsilon_0\chi_1(\omega)+\varepsilon_0\chi_3(\omega)I],\end{aligned} \tag{18}$$

where μ_0 is the permeability of the material, I is the incident light intensity, ε_r is the real part of the dielectric constant, and $\chi_1(\omega)$ and $\chi_3(\omega)$ refer to the linear and nonlinear contribution to the polarization with the same frequency of the incident field.

The expression for the linear optical absorption coefficient is given by

$$\alpha_1(\omega) = \frac{4\pi\alpha_f\sigma_s}{n_r e^2}\hbar\omega|M_{fi}|^2\delta(E_f-E_i-\hbar\omega), \tag{19}$$

and the nonlinear optical absorption coefficient is expressed as

$$\begin{aligned}\alpha_3(\omega,I) = &-\frac{32\pi^2\alpha_f\sigma_s I}{n_r^2e^2\hbar\Gamma_{ff}}\hbar\omega|M_{fi}|^2\delta(E_f-E_i-\hbar\omega)\\ &\times\Big\{1-\frac{|M_{ff}-M_{ii}|^2}{4|M_{fi}|^2}\\ &\times\frac{[(\hbar\omega-E_{fi})^2-(\hbar\Gamma_{fi})^2+2E_{fi}(E_{fi}-\hbar\omega)]}{E_{fi}^2+(\hbar\Gamma_{fi})^2}\Big\},\end{aligned} \tag{20}$$

where n_r is the refractive index of the material that we have taken, σ_s is the electron density of the quantum dot, ω is the angular frequency of the incident photon energy, α_f is the fine structure constant, and E_i and E_f denote the confinement energy levels for the ground and the first excited states, respectively.

From Eqs. (19) and (20), the energy-conserving delta function by the Lorentzian is given by

$$\delta(E_f-E_i-\hbar\omega) = \frac{\Gamma}{\pi\{(E_f-E_i-\hbar\omega)^2+\Gamma^2\}}, \tag{21}$$

where Γ is the line width of the exciton. Here, the value, $\Gamma = 0.1$ meV, is taken into consideration. Further, the homogeneous spectral width due to the finite coherence time between the two energy levels is also taken into account for the calculations.

The susceptibilities are related to the refractive index changes as

$$\frac{\Delta n(\omega)}{n_r} = \mathrm{Re}\Big[\frac{\chi(\omega)}{2n_r^2}\Big], \tag{22}$$

where n_r is the refractive index of the material. The analytic expressions of the linear and nonlinear changes in the refractive index are given by[31]

$$\frac{\Delta n_{(1)}(\omega)}{n_r} = \frac{\sigma_s e^2}{2\varepsilon_r}|M_{fi}|^2\frac{\hbar\omega_{fi}-\hbar\omega}{(E_{fi}-\hbar\omega)^2-(\hbar\Gamma_{fi})^2} \tag{23}$$

and

$$\begin{aligned}\frac{\Delta n_{(3)}(\omega)}{n_r} = &-\frac{\mu_0 cI}{4\varepsilon_r n_r^2}\frac{\sigma_s e^4|M_{fi}|^4}{[(E_{fi_i}-\hbar\omega)^2+(\hbar\Gamma_{fi})^2]^2}\\ &\times 4|M_{fi}|^2(E_{fi}-\hbar\omega)-\Big\{|M_{ff}-M_{ii}|^2\\ &\times\frac{[(E_{fi}(E_{fi}-\hbar\omega_{fi})^2-(\hbar\Gamma_{fi})^2(3(E_{fi}-2\hbar\omega)]}{E_{fi}^2+(\hbar\Gamma_{fi})^2}\Big\}.\end{aligned} \tag{24}$$

Hence the total refractive index change is given by

$$\frac{\Delta n(\omega)}{n_r} = \frac{\Delta n_{(1)}(\omega)}{n_r}+\frac{\Delta n_{(3)}(\omega)}{n_r}. \tag{25}$$

The third-order nonlinear optical susceptibility $\chi(3)$ related to the optical mixing between two incident light beams with different frequencies (ω_1 and ω_2) is expressed as[32,33]

$$\begin{aligned}&\chi^3(-2\omega_1+\omega_2;\omega_1,-\omega_2)\\ &= -\frac{2\mathrm{i}Ne^4|\mu|^4}{\varepsilon_0\hbar^3}\frac{1}{[\mathrm{i}(\omega_0-2\omega_1+\omega_2)+\Gamma][\mathrm{i}(\omega_2-\omega_1)+\Gamma]}\\ &\times\Big[\frac{1}{[\mathrm{i}(\omega_0-\omega_1)+\Gamma]}+\frac{1}{[\mathrm{i}(\omega_2-\omega_1)+\Gamma]}\Big],\end{aligned} \tag{26}$$

where μ refers to the dipole matrix element, defined as the transition frequency $\omega_0 = (E_f-E_i)/\hbar$, and N is the number of charge carriers.

3. Results and discussion

A parabolic InAs quantum dot embedded in a GaAs material is considered in this problem. The results are obtained for exciton binding energy, interband emission energy, Landé factor, and some nonlinear optical properties in a $Ga_{0.2}In_{0.8}As$/GaAs-strained quantum dot in the presence of magnetic field strength. The heavy hole mass has been used throughout our calculations, for the heavy excitons are more common in experiment. The confinement potential includes the strain effect. The atomic units are adopted in determining electronic charges and wave functions in which the electronic charge and Planck's constant are both assumed to be unity. The measure of magnetic field, one gamma represents 0.497 T.

Figure 1 shows the plots of exciton binding energy versus dot radius of $Ga_{0.2}In_{0.8}As$/GaAs quantum dot for various magnetic field strengths. The inset shows the corresponding diamagnetic shifts of binding energy versus magnetic field strength for three different dot radii of $Ga_{0.2}In_{0.8}As$/GaAs quantum dot. It is observed that the exciton binding energy strongly depends on magnetic field strength and geometrical confinement. The exciton binding energy is observed to in-

crease with the geometrical size of the quantum dot decreasing. It is because the relative distance between the electron and the hole decreases and the Coulomb interaction between them is increased. The exciton binding energy still decreases for the strong spatial confinement, which is due to the nature of unbound of exciton in that region.[34] Further, it is noticed that the exciton binding energies are found to increase with magnetic field strength increasing for all the quantum dot radii, however, the increase in exciton binding energy is less sensitive for smaller dot radii. But the spatial confinement dominates over the effects of magnetic field for the smaller dot radii. On the contrary, the effects of magnetic field strength are found to be more prominent when the dot radius increases. The more nonlinear behavior for the larger dot is observed in the insert in which the diamagnetic shifts increase with magnetic field strength increasing for three different dot radii. We present the variations of magnetic field-induced interband emission energy with dot radius in a $Ga_{0.2}In_{0.8}As/GaAs$ quantum dot in Fig. 2. It is observed that the interband optical transition energy is enhanced with the dot radius decreasing. And the effect is more pronounced for the strong confinement.

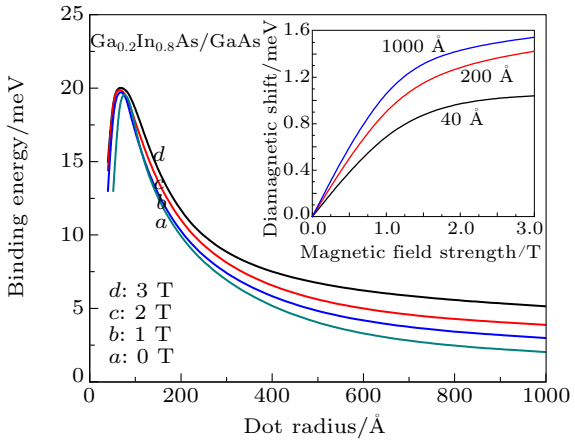


Fig. 1. (color online) Variations of exciton binding energy with the dot radius of a $Ga_{0.2}In_{0.8}As/GaAs$ quantum dot for various magnetic field strengths. The insert shows the corresponding diamagnetic shifts of binding energy as magnetic field strength increases for three different dot radii of a $Ga_{0.2}In_{0.8}As/GaAs$ quantum dot.

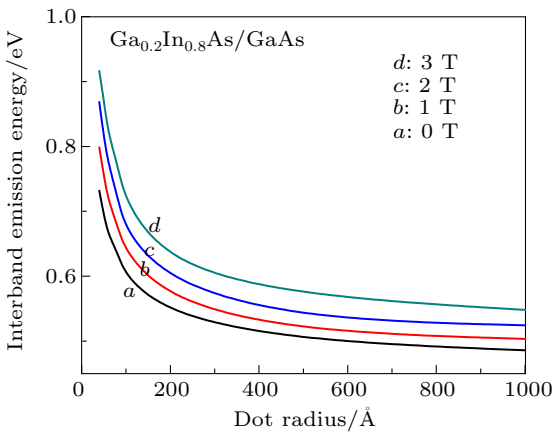


Fig. 2. (color online) Variations of magnetic field-induced interband emission energy with dot radius for various magnetic field strengths in a $Ga_{0.2}In_{0.8}As/GaAs$ quantum dot.

In Fig. 3, we show the variations of electron (hole) g-factor with dot radius for various magnetic field strengths in a $Ga_{0.2}In_{0.8}As/GaAs$ quantum dot. The variation of the effective g-factor as a function of the band gap is obtained from the bulk formula.[35] It is noticed that the effective electron (hole) g-factor approaches to the bulk g value of InAs when the dot radius decreases but the g-factor tends to become the bulk values of the g-factor of GaAs for larger dot sizes. The effects of the magnetic field make the values of the Landé factor increase. The magnitude of the hole g-factor seems to be larger than that of the electron g-factor. It is noted that the effective electron (hole) g-factor is enhanced with dot radius increasing.[36]

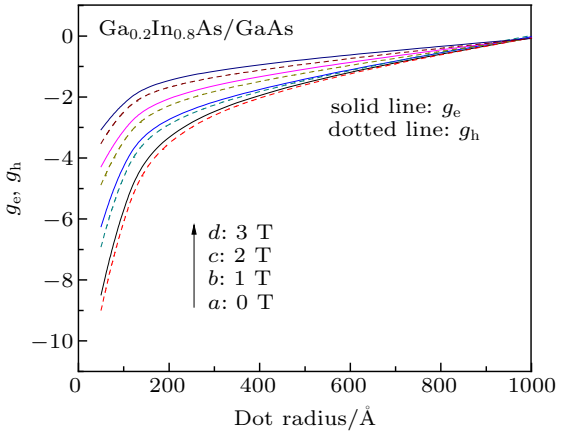


Fig. 3. (color online) Variations of electron (hole) g-factor with dot radius for various magnetic field strengths in a $Ga_{0.2}In_{0.8}As/GaAs$ quantum dot.

We present the variations of theoretical exchange enhancement with dot radius for various magnetic field strengths in a strained $Ga_{0.2}In_{0.8}As/GaAs$ quantum dot in Fig. 4. The exchange enhancement of J with respect to the bulk value of exciton in the quantum dot is brought out here by considering the overlap integral between electron and hole wave functions. It is noticed that the exchange enhancement is enhanced as dot radius decreases. The exchange enhancement is found to increase as exciton confinement increases. A sudden decrease in exchange enhancement is observed in the weak confinement region due to the tunneling of the wave function through the barrier. A similar behavior has been investigated earlier for GaAs and InGaAs quantum wells.[37] It is observed that the exchange splitting energy increases as dot radius decreases and it is more pronounced for smaller dots. And this energy increases as the alloy content value increases due to the strain contribution and the geometrical confinement for the smaller dots, and the results qualitatively resemble the previous results.[37]

Figure 5 shows the variations of oscillator strength with dot radius for various magnetic field strengths in a strained $Ga_{0.2}In_{0.8}As/GaAs$ quantum dot. The oscillator strengths are

observed to increase with dot radius increasing for all the magnetic field strengths. From Eqs. (15) and (16), it follows that the oscillator strength purely depends on effective mass, consequently the smaller the effective mass, the larger the oscillator strength. The radiative exciton lifetime decreases with dot radius increasing. Thus, the oscillator strength is expected to decrease as the quantum size effect is dominant.

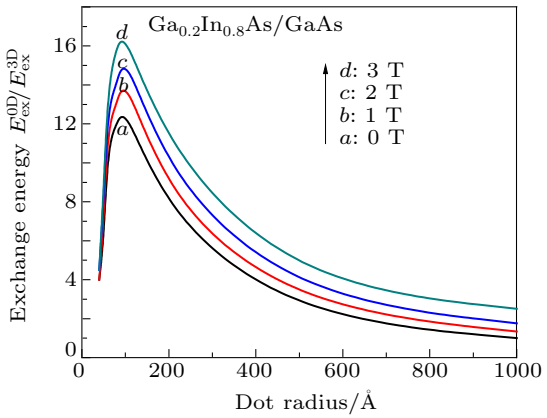


Fig. 4. (color online) Variations of theoretical exchange enhancement with dot radius for various magnetic field strengths in a strained $Ga_{0.2}In_{0.8}As/GaAs$ quantum dot.

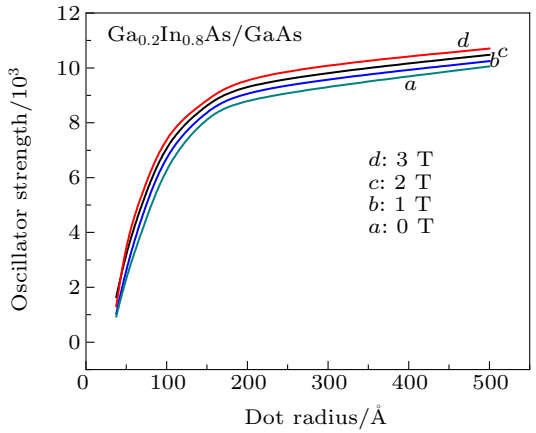


Fig. 5. (color online) Variations of oscillator strength as a function of dot radius for various magnetic field strengths in a strained $Ga_xIn_{1-x}As/GaAs$ quantum dot.

Figure 6 shows the variations of total absorption coefficient of an exciton with photon energy in a strained $Ga_{0.2}In_{0.8}As/GaAs$ quantum dot with a 50-Å dot radius for different values of magnetic field strength. It is observed that the absorption coefficient peak shifts towards the higher photon energy as the magnetic field increases with the value of absorption coefficient decreasing. The results show that resonant peak shifts towards the blue region under an applied magnetic field. It is because that the spacing between the energy levels increases with additional confinement due to the magnetic field.[38] Dipole matrix element and the difference between the energies are two important parameters involved in calculating the oscillator strength. When the energy of photon is equal to the intersubband transition energy, a large value of dipole matrix element occurs, and the dielectric constant of the semiconductor material eventually changes the index of refraction and absorption coefficient. It can be attributed to the enhancement of nonlinear optical property.

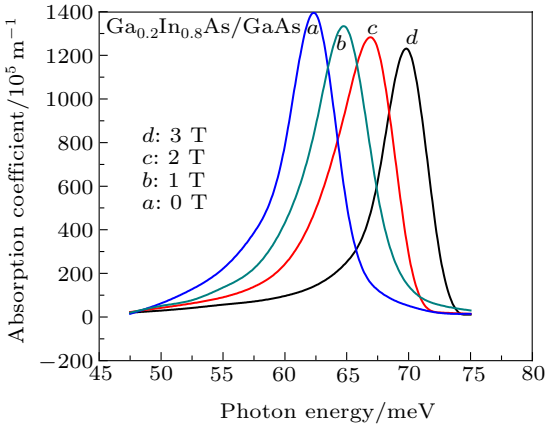


Fig. 6. (color online) Variations of the total absorption coefficient of an exciton with photon energy in a strained $Ga_{0.2}In_{0.8}As/GaAs$ quantum dot with a 50-Å dot radius for different values of magnetic field strength.

In Fig. 7 the variations of change of refractive index with photon energy are presented for different magnetic field strengths in a $Ga_{0.2}In_{0.8}As/GaAs$ with a constant dot radius of 50 Å. The refractive index is related generally to the intersubband transition energy and it contains two components of the refractive index, namely linear and nonlinear terms. We have observed that the change of refractive index increases with magnetic field strength. Also, it is observed from Eqs. (19) and (20) that the linear relative change of the refractive index does not depend on photon intensity but the third-order relative change of the refractive index changes with photon intensity and it varies quadratically with the matrix element of the electric dipole moment of the transition. Thus, the nonlinear term must be considered when calculating the refractive index change of quantum dot systems.[39]

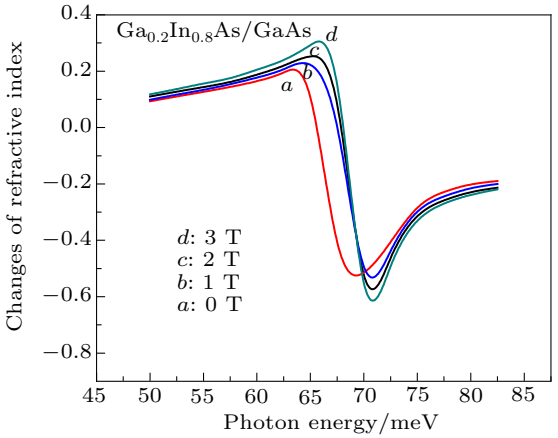


Fig. 7. (color online) Variations of refractive index changes with photon energy for three different magnetic field strengths in a $Ga_{0.2}In_{0.8}As/GaAs$ with a constant dot radius of 50 Å.

Figure 8 displays the variations of third-order susceptibility of the third harmonic generation with photon energy under different magnetic field strengths in a $Ga_{0.2}In_{0.8}As/GaAs$ quantum dot with $\hbar\omega_0 = 50$ meV. It is observed from the figure that the resonant peaks occur twice. It is known that the relaxation time has a stronger dependency on the third-order susceptibility. The magnitude of the third-order susceptibility is found to be higher for longer relaxation times. Further, it is found that the magnitude of the third-order susceptibility of third-order harmonic generation increases with magnetic field strength increasing. Eventually, the damping factor determines the lifetime of the exciton in the confined state.[40] Hence it is concluded that the relaxation time and the external magnetic field strength have a greater influence on the third-order susceptibility of the third harmonic generation.

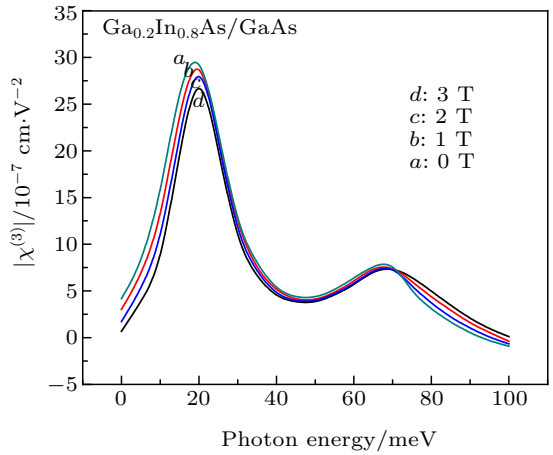


Fig. 8. (color online) Variations of the third-order susceptibility of the third harmonic generation with photon energy for different magnetic field strengths in a $Ga_{0.2}In_{0.8}As/GaAs$ quantum dot with $\hbar\omega_0 = 50$ meV.

4. Conclusions

In this paper, the heavy hole excitonic states and some nonlinear optical properties in a strained $Ga_{0.2}In_{0.8}As/GaAs$ quantum dot have been discussed in the presence of magnetic field strength. The anisotropy, non-parabolicity of the conduction band, and the geometrical confinement are taken into account in the calculations. The magnetic field dependence of effective excitonic g-factor as a function of dot radius is investigated numerically. The interband optical transition energy as a function of magnetic field strength and spatial confinement is obtained. The oscillator strengths of interband transition under the geometrical confinement, the heavy hole excitonic absorption spectra, changes of refractive index, and the third-order susceptibility of the third harmonic generation are obtained under various magnetic field strengths in the $Ga_xIn_{1-x}As/GaAs$ quantum dot. We believe that the obtained optical results can stimulate further research work on optical devices such as infrared red lasers.

References

[1] Peng J and Li S S 2012 *Chin. Phys. Lett.* **29** 047301
[2] Ramvall P, Tanaka S, Nomura S, Riblet P and Aoyagi Y 1998 *Appl. Phys. Lett.* **73** 1104
[3] Sidor Y, Partoens B and Peeters F M 2005 *Phys. Rev. B* **71** 165323
[4] Cusack M A, Briddon P R and Jaros M 1998 *Physica B* **253** 10
[5] Li M F, Tian X and Zhao Z Y 2004 *Chin. Phys.* **13** 1649
[6] Tan N and Zhang Q Y 2006 *Chin. Phys.* **15** 2165
[7] Ridha P, Li L, Fiore A, Patriarche G, Mexis M and Smowton P M 2007 *Appl. Phys. Lett.* **91** 191123
[8] Li S S, Chang K and Xia J B 2005 *Phys. Rev. B* **71** 155301
[9] Xu X and Feng Y P 2003 *J. Phys. Chem. Solids* **64** 2301
[10] Preisler V, Grange T, Ferreira R, De Vaulchier L A, Guldner Y, Teran F J, Potemski M and Lemaitre A 2009 *Eur. Phys. J. B* **67** 51
[11] Offermans P, Koenraad P M, Wolter J H, Pierz K, Roy M and Maksym P A 2005 *Phys. Rev. B* **72** 165332
[12] Grundmann M, Stier O and Bimberg D 1995 *Phys. Rev. B* **52** 11969
[13] Tangarife E and Duque C A 2010 *Appl. Surf. Sci.* **256** 7234
[14] Stier O, Grundmann M and Bimberg D 1999 *Phys. Rev. B* **59** 5688
[15] Shen W Z 2001 *Appl. Phys. Lett.* **79** 1285
[16] Shen W Z, Tang W G, Shen S C, Wang S M and Andersson T G 1994 *Appl. Phys. Lett.* **65** 2728
[17] Shen W Z, Shen S C, Tang W G, Wang S M and Andersson T G 1995 *J. Appl. Phys.* **78** 1178
[18] Herbert Li E 2000 *Physica E* **5** 215
[19] Singh J 1996 *Optoelectronics: An Introduction to Materials and Devices* (New Delhi: Tata McGraw Hill)
[20] Nolte D D, Walukiewicz W and Haller E E 1987 *Phys. Rev. Lett.* **59** 501
[21] Adachi S 1992 *J. Appl. Phys.* **53** 8775
[22] Krijn M P C 1991 *Semicond. Sci. Technol.* **6** 27
[23] Frogley M D, Downers J R and Dunstan D J 2000 *Phys. Rev. B* **62** 13612
[24] Duque C A, Porras-Montenegro N, Barticevic Z, Pacheco M and Oliveira L E 2006 *J. Phys.: Condens. Matter* **18** 1877
[25] Bir G L and Pikus E 1974 *Symmetry and Strain-Induced Effects in Semiconductors* (New York: Wiley)
[26] Scriba J, Wixforth A, Kotthaus J P, Bolognesi C R, Nguyen C and Kroemer H 1993 *Solid State Commun.* **86** 633
[27] Revathi M, Chang K Y and John P A 2010 *Physica E* **43** 322
[28] Koga T, Nitta J, Takayanagi H and Datta S 2002 *Phys. Rev. Lett.* **88** 126601
[29] Vladimir A Fonoberov and Alexander A Balandin 2004 *Appl. Phys. Lett.* **85** 5971
[30] de Sousa J S, Leburton J P, Freire V N and da Silva E F 2005 *Phys. Rev. B* **72** 155438
[31] Sali A, Satori H, Fliyou M and Loumrhari H 2002 *Phys. Status Solidi (b)* **232** 209
[32] Takagahara T 1987 *Phys. Rev. B* **36** 9293
[33] Liang S J and Xie W F 2011 *Physica B* **406** 2224
[34] Minimala N S and John P A "Effects Of Magnetic Field and the Built-in Internal Fields on the Absorption Coefficients in a Strained Wurtzite GaNAlGaN Quantum Dot", 2013 *AIP Conf. Proc.* **1512** 1012
[35] Pryor Craig E and Flatté, Michael E 2006 *Phys. Rev. Lett.* **96** 026804
[36] Hendorfer G and Schneider J 1991 *Semicond. Sci. Technol.* **6** 595
[37] Chen Y, Gil B, Lefebvre P and Mathieu H 1988 *Phys. Rev. B* **37** 6429
[38] Xie W F 2009 *Commun. Theor. Phys.* **52** 155
[39] Yu Z G and Srini K 2006 *J. Opt. Soc. Am. B* **23** 2356
[40] Duque C M, Mora-Ramos M E and Duque C A 2011 *J. Nanopart. Res.* **13** 6103